MECHANISMS OF SILICON AMORPHIZATION AT THE ULTRASOUND ACTION DURING ION IMPLANTATION

B. ROMANYUK, D. KRÜGER[1]**, V. MELNIK, V. POPOV, E. BORSHCHAGOVSKYI, Ya. OLIKH, V. SOROKA**[2]

Institute for Semiconductor Physics, Nat. Acad. of Sci. of Ukraine
(*Prosp. Nauki, 45, Kyiv 03022, Ukraine*),
[1] Institute for Semiconductor Physics
(*W. Korsing Str., 2, Frankfurt (Oder) 15230, Germany*),
[2] Institute for Nuclear Research, Nat. Acad. of Sci. of Ukraine
(*Prosp. Nauki, 47, Kyiv 03022, Ukraine*)

UDC 621.382
‰ 2001

The present study aims to investigate the ultrasound-dependent silicon amorphization during ion irradiation to determine the effect of point defect out-diffusion on the kinetics of the amorphization process in more detail. We show that the defect density in the surface layer and the thickness of an amorphous layer increase by the *in situ* US treatment. We discuss the results in frames of the point defect separation and out-diffusion model.

Ion implantation of the crystalline silicon produces a damage of the crystal lattice. Under certain experimental conditions, this effect leads to the phase transformation from the crystalline to amorphous phase. Implantation-induced amorphization is widely applied to reduce channeling tales of dopant profiles during integrated circuit manufacturing [1]. The study of amorphization has a fundamental significance for the radiation physics of solids. In traditional models, amorphization is occurred when isolated damaged regions created by individual ions overlap, or via the build-up of point defects, leading to a collapse of a region of silicon into the amorphous phase [2]. Damaged regions are formed along a single ion track as a result of quenching the collision cascade [3]. The out-diffusion of point defects from damaged regions is of a great importance for the kinetics of amorphization [4]. Despite numerous studies, the mechanisms of amorphization by ion implantation are still under intensive debates [5, 6]. This is related to the necessity to take numerous factors into account, e.g., ion current densities, ion masses, substrate temperatures, and presence of additional factors as electrical or mechanical fields [7]. It was suggested that ultrasonic (US) waves propagating through the semiconductor can affect the generation of point defects and dissociation of defect complexes [8]. In this connection, it seems to be perspective to use *in situ* ultrasonic treatments during the implantation process, when target atoms are in an excited state, and defect complexes are unstable.

The present study aims to investigate the ultrasound-dependent amorphization during ion irradiation of silicon to determine the effect of point defect out-diffusion on the kinetics of amorphization in more detail. We show that the defect density in the surface layer and the thickness of the amorphous layer increase by the US treatment. We discuss the results in frames of the point defect separation and out-diffusion model.

Experimental

Boron-doped 10 Ohm · cm Czochralsky-grown (Cz-Si) Si wafers, (100), were mounted inside the implantation chamber onto piezoelectric transducers via special acoustic binder. Low-amplitude US vibrations were generated in the wafer by means of a transducer operating in the resonance vibration mode. We varied the basic resonance frequency from 600 kHz to 7 MHz. The amplitude of acoustic strain did not exceed 10^5 corresponding to an acoustic power of $1\,\mathrm{W/cm^2}$. For implantation, we used Ar^+ ions with energies of 150 keV and doses from $1 \cdot 10^{13}$ to $1 \cdot 10^{15}\,\mathrm{cm}^{-2}$. The ion flux was $6 \cdot 10^{10}$ to $3 \cdot 10^{12}$ ion $/\,\mathrm{cm}^2$.

Rutherford backscattering spectrometry (RBS) combined with channeling was employed for damage studies. Measurements were performed by ⟨100⟩ channeling of 1.5 MeV helium ions at a scattering angle of 170°. Determination of the amorphous layer thickness

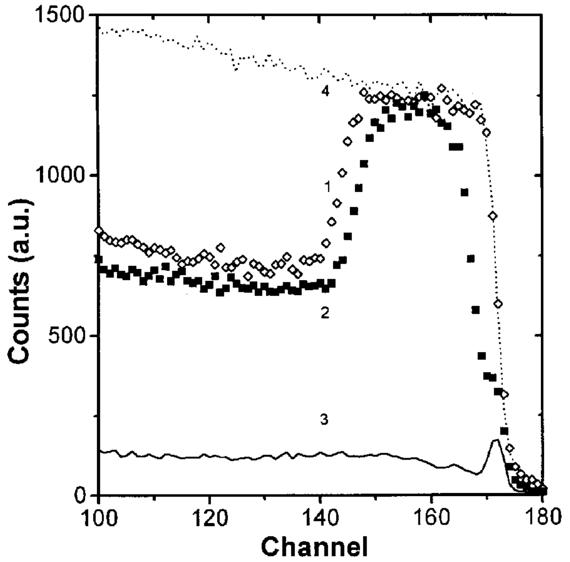

Fig.1. RBS spectra for implanted samples: *1* — with US treatment; *2* — without US treatment; *3* — initial sample before implantation; *4* — random spectrum

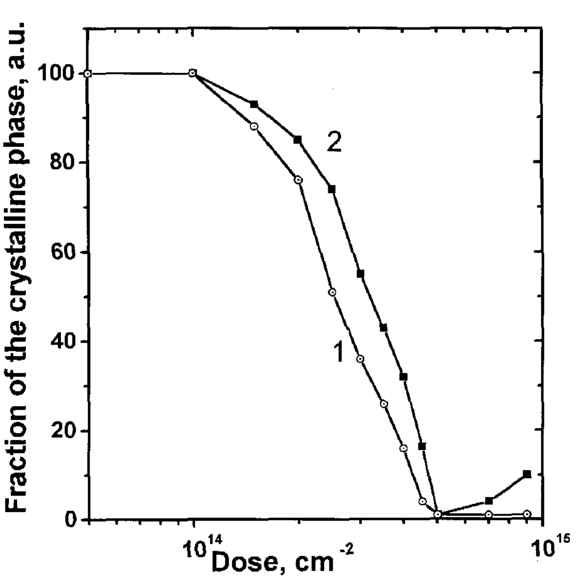

Fig.2. Dose dependences of the fraction of the crystalline phase for silicon: *1* — with US treatment; *2* — without US treatment

from RBS spectra was carried ont taking an approach generalized in [8].

The implanted structures were studied by the multi-angle spectral ellipsometry method within the spectral range 225 to 1200 nm and the range of angles of incidence 60 to 80°. Thus, the measured parameters are ellipsometric angles Ψ and Δ describing a relative change of amplitude and phase under different conditions of polarization. The *p*- and *s*-polarized components, i.e., light polarized in the plane of incidence and perpendicular to it are standardly used. These angles are connected with parameters of the structure investigated through the basic equation of ellipsometry:

$$\mathrm{tg}\Psi \exp(i\Delta) = r_p/r_s,$$

where r_p and r_s designate the amplitude factors of reflection for appropriate polarizations.

As the factors of reflection are complex functions of the system parameters, the processing of the results of measurements were carried out numerically using optimization methods for solving the inverse problem. Thus, the determined parameters of the chosen model were varied for the adjustment of the measured values and calculated ones by the method of least squares. To account the refraction factors of composite materials, the models of effective medium approximation [9] are widely used. Most common one, if there are no physical preferences for other models, is the model based on the self-coordinated account of a local field in a mixture. Thus, the optical parameters of components have to be undertaken or from the preliminary measurements of pure materials, or from the existing directories of optical constants.

Results

In Fig.1, the RBS spectra are shown for implanted samples with (curve *1*) and without (curve *2*) ultrasonic treatment during ion implantation. For comparison, the spectrum of an initial samle (before ion implantation, curve *3*) and a random spectrum (curve *4*) are given also. The thickness t of the amorphous layer can be found from the energy width ΔE taken from the full width at half-heights of the signal from the amorphous layer: $\Delta E = [\varepsilon]Nt$, where $[\varepsilon]$ — backscattering stopping cross section factor, N — atomic density of the target. The dose dependences of fraction of the crystalline phase at implantation with and without US treatment, determined according to the technique in [10], are given in Fig.2.

In Fig.3, the typical results of ellipsometric measurements of the Ψ and Δ parameters for a sample with US treatment are given. In the same figure, the continuous curves give the results of computer modeling of the Ψ and Δ spectra for the parameters of surface disordered layers appropriate to the optimum coordination of the theory and experiment.

The data on structure and thickness of superficial layers obtained from the RBS and ellipsometry data are summarized in Table.

In Fig.4, we present superficial sublayers tested by the ellipsometry method, whose structure and thickness are given in Table. In the same figure, the distribution of radiation defects, generated during ion implantation (using the TRIM-98 program), is given.

As follows from the data of Fig.1, the *in situ* US treatment during ion implantation essentially influences the structure (defectness) of the surface area of silicon. Without US treatment, there exists a layer (~ 18nm) of defective monocrystalline Si at the surface and a buried amorphous layer. But, in the case of ultrasound influence, the completely amorphized silicon layer starts directly from the surface. In addition, the total thickness of the amorphous layer is approximately by 1.3 times more than that in the case of US treatment.

The data of ellipsometry allow one to obtain the more detailed information on the structure of the subsurface Si layer and, as is visible from Table and Fig.4, on the whole, confirm the resutls obtained from the analysis of the RBS spectra. A distinction in the total thickness of disordered layers from the RBS and ellipsometry data is explained by the presence of extended lightly-disordered layers (area *5* in Fig. 4,*a* and area *2* in Fig.4,*b*). Such areas are well distinguished by ellipsometry researches, but practically are not fixed by the RBS method.

Discussion

We propose that US induced enhanced amorphization can be modelled in terms of US stimulated diffusion of interstitial, decreased recombination of point defects and kinetic changes in vacancy complex formation.

Summarized data on structure and subsurface layer thickness according to RBS and ellipsometry measurements

US treatment during implantation	With US treatment. $P = 1\,\mathrm{W/cm^2}$	Without US treatment
Thickness of disordered layers (**RBS data**)		
Total	**224 nm**	**176 nm**
Including:		
1	a-Si	c-Si + a-Si
2	a-Si + c-Si	a-Si
3	c-Si (substrate)	a-Si + c-Si
4		c-Si (substrate)
Thickness of disordered layers (**ellipsometry data**)		
Total	**347 nm**	**228 nm**
Including:		
1	Surface SiO_2 5.37 nm	Surface SiO_2 6.48 nm
2	a-Si + 8.7% voids 59.74 nm	c-Si + 41.2% a-Si 17.76 nm
3	a-Si + 16.1% voids 55.03 nm	a-Si 74.88 nm
4	a-Si + 34.5% voids 145.39	a-Si + 22% voids 134.69
5	c-Si + 45.6% a-Si + 14.9% voids 87.03 nm	c-Si (substrate)
6	c-Si (substrate)	

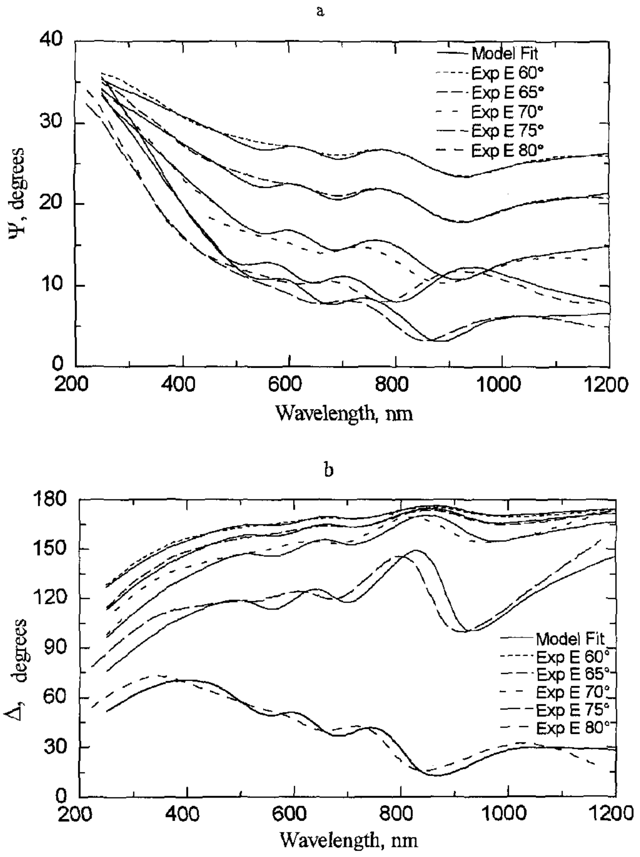

Fig.3. Results of ellipsometry measurements and the computer simulation data (solid lines) for the implanted sample with US treatment

In the case of Ar^+ implantation, every ion creates a disordered area with a diameter of about 3 to 6 nm [11]. Subsequently, cascade cooling, partial recombination of point defects, and creation of point defect complexes occur. Estimations show that, for a transition into the amorphous state, approximately 14 percent of atoms have to be displaced from their lattice sites. If the implantation dose increases, amorphous areas grow due to absorption of point defects up to overlapping and formation of a continuous amorphous layer.

The presence of US waves with a moderate intensity (0.1 to 1.0 $\mathrm{W/cm^2}$) and a frequency in the range 0.6 – 7 MHz in the crystal lattice generates substantially less energy in comparison to that, transferred to lattice atoms by the incident ion beam. Therefore, the given UST should not influence the point defect generation.

Our experiments indicate that US excitation during ion implantation increases the amorphous layer thickness and reduces the critical amorphization dose

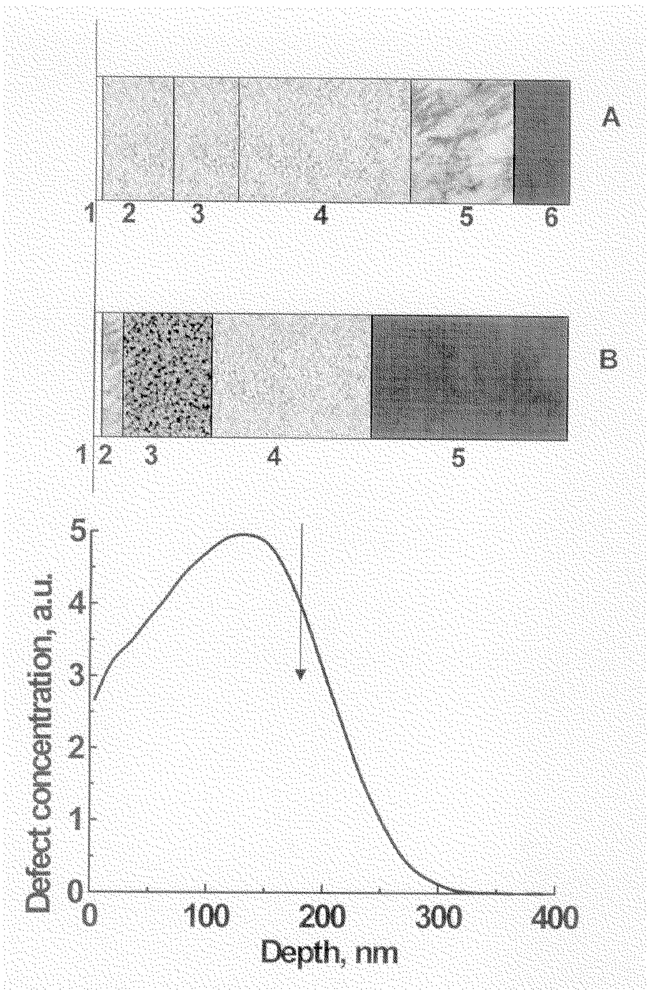

Fig.4. Schematic presentation of disordered layers by the ellipsometry data (*A* — with US treatment, *B* — without US treatment) and TRIM simulation of the radiation point defect depth profile. Arrow indicates the R_p position for the implantation regime used

(see Fig.2). Obviously, the used US intensity under the non-equilibrium conditions of ion irradiation causes crucial changes. In the absence of ion irradiation, we could not detect any changes in the crystal from the sound field alone.

We established that UST at 2 MHz results in a movement of the outer a-c interface towards the surface, where vacancy defects are usually accumulated. We suppose, in analogy to a model of US gas bubbles cavitation in liquids [12], that UST stimulates the following processes during implantation: a) coupling of vacancies into complexes; b) tension-compression of formed 'vacancy bubbles“ under US waves resulting in their deformation, growth, and movement to the surface, c) formation of Ar bubbles. This enhances the overlapping of disordered regions and stimulates the formation of a continuous amorphous layer up to the surface.

An absorption of phonons generated by US waves with frequencies in the range 0.6 – 7 MHz by the lattice will lead only to a small lowering of the activation energy for diffusion. However, a low-frequency US wave can excite also high frequency phonons in the lattice as a result of non-linear processes [13]. An absorption of these phonons seems to be significant for diffusion enhancement [14].

The processing of the results of ellipsometry measurements has confirmed the data received from the RBS and model representation stated above. Spectra in implanted samples without ultrasonic treatment are described by a more simple model, Fig.4,*b*, which contains a buried layer of amorphous silicon (which is approximated by the two-layer model with and without voids) — layers *3*, *4* in Fig.4,*b*, and also a subsurface partially amorphized layer (*2*). The spectra received on samples, implanted with influence of ultrasound, are described by a more complex model. It includes several sublayers, and the general thickness of the disordered area is more essential. The superficial crystal layer is absent and there is a defective crystal layer on the internal interface with not damaged volume (Fig.4,*a*).

The highly exact description of data requires the introduction of voids in the model. Such voilds are needed for the account of vacancy clustering or creation of microbubbles of implanted argon. Without US treatment during implantation, the greater fraction of interstitials and vacancies annihilate, and voids localized near the R_p (layer *4* in Fig. 3,*b*) are caused by Ar bubbles. In samples, implanted with US influence, the accelerated out-diffusion of interstitial atoms from the region of their maximal concentration (near R_p) into the bulk of a sample takes place. It decreases the interstitial/vacancy recombination. As a result, the thickness of the amorphous region enriched by vacancies and their complexes (voids) is increased, and there is an additional defective sublayer on the internal interface of the amorphous layer (layer *5* in a Fig. 4,*a*). As a most probable reason for the occurrence of such a layer, we consider the formation of complexes of interstitial atoms.

Conclusions

We have investigated, for the first time, the effect of *in situ* ultrasound treatment during ion implantation on amorphization of crystalline silicon. A strong influence is found. RBS-C and ellipsometry measurements have demonstrated that the appropriate ultrasound treatment enhances amorphization of Si during Ar implantation, especially at lower US frequencies (near 2 MHz). The effect depends on ion flux and ultrasound frequency. The experimentally observed effects are discussed in terms of US-stimulated enhanced point defect diffusion, interaction, and clustering.

We would like to thank Prof. V. Litovchenko and Prof. A. Ourmazd for helpful discussions.

This paper was supported by the BMBF project 01M2976.

1. *Dennis J.R., Hale E.B.*//J. Appl. Phys. ¯ 1978. ¯ **49**, N3. – P.1119 ¯ 1121.
2. *Thornton J., Webb R.P., Wilson I.H., and Paus K.S.*//Semicond. Sci. and Technol. ¯ 1988. ¯ **3**, N5. ¯ P.281 ¯ 285.
3. *Moreheed F.F., Crowder B.L.*//Radiat. Effects. ¯ 1980. ¯ **25**, N5. ¯ P.49 ¯ 54.
4. *Ion* Implantation and Beam Processing. // Ed.by J.S. Williams and J.M. Peate. ¯ New Nork: Acad. Press, 1984. ¯ P .19 ¯ 52.
5. *Goldberg R.D., Williams J.S., Elliman R.G.* // Nucl. Instrum. and Meth. in Phys. es. B. ¯ 1995. ¯ **106.** ¯ P. 242 ¯ 246. –
6. *Goldberg R.D., Elliman R.G., Williams J.S.*//Ibid. ¯ 1993. – **80/81** , N3. ¯ P.596 ¯ 599.
7. *Campisano S.U., Coffa S., Raineri V. et al.*//Ibid. ¯ P.514 ¯ 518.
8. *Ostrovskii I.V., Lysenko V.N.*//Sov. Phys. Solid State. ¯ 1982. ¯ **24**, N4. ¯ P.682 ¯ 683.
9. *Aspnes D.E.*//Thin Solid Films. ¯ 1982. ¯ **89**, N2. ¯ P.249 ¯ 262.
10. *Mayer J.W., Rimini E.* Ion Beam Handbook for Material Analysis. ¯ New York: Acad. Press, 1997.
11. *Gotz G., Glaser E., Wesch W., Sobolev N.*//Proc. Intern. Conf. 'Rad. Phys. of Semicond“. Tbillisi, Georgia, Sept. 13 ¯ 19, 1979. ¯ P.391 ¯ 396.
12. ¥•£‡ · . // †Œ́ §¢°– ¤ ¥£µ ¶•¤‡¥·¥·¤¥ ¢ ·°–¥ ¤ É¥Ì·¤-–¥/ µ́ •¥⁄. . . •¤£µÓ¥¢ . ¯ .: §⁄-¢µ ·µÉ. †¤É, 1956. ¯ .501 ¯ 511.
13. *Pavlovich I.V.*//Phys. status solidi (b). ¯ 1993. ¯ **180**, N1. ¯ P.97 ¯ 105.
14. *Olikh Ya.M. and Shavlyuk Yu.N.*//Sov. Phys. Solid State. ¯ 1996. ¯ **38**, N11. ¯ P.1835 ¯ 1838.

Received 09.12.99